GMR Genetics and Molecular Research
Online Journal
ISSN:1676-5680

Determination of patellar ligament and anterior cruciate ligament geometry using MRI

H.P. Wang[1], H.K. Cui[2], W. Yue[1], R.F. Yan[1], J.P. Ren[1], Z.S. Zhai[1], C.H. Liang[1], R.M. Yang[1] and D.M. Han[1]

[1]Image Center, The First Affiliated Hospital of Xinxiang Medical University, Weihui City, China
[2]Department of Gynaecology and Obstetrics, The First Affiliated Hospital of Xinxiang Medical University, Weihui City, China

Corresponding author: D.M. Han
E-mail: ruiminyangcn@163.com

Genet. Mol. Res. 14 (4): 12352-12361 (2015)
Received January 23, 2015
Accepted May 6, 2015
Published October 16, 2015
DOI http://dx.doi.org/10.4238/2015.October.16.1

ABSTRACT. Ligament geometry is crucial to surgical treatment success in anterior cruciate ligament (ACL) injury. This study aimed to optimize the MRI technique to elucidate the geometry of the patellar ligament (PL) and ACL *in vivo*. A 1.5-T superconducting MRI system with a special surface coil and fast spin echo was used to acquire high-resolution T1-weighted images (H-T1WI) of the ACL. The sagittal plane angle was 10° to 15° towards the inner side of the vertical line of the tangent line axis of the femoral intercondylar fossa. The H-T1WI images of the PL were centered at the lower margin of the patella and the center of the tibial tuberosity. The lengths of the PL and ACL were measured using a Radworks 5.1 workstation. ACL and PL lengths were compared between left and right knees and between genders, and left PL length measurements obtained separately by three doctors underwent correlation analysis. The quality of the images satisfied the clinical measurement requirements. The duration of sagittal image acquisition was 2 min and 25 s. The average PL length was 42.20 ±

4.21 and 40.15 ± 4.00 mm, and the average ACL length was 36.98 ± 4.12 and 35.80 ± 4.67 mm, in male and female subjects, respectively. The intraclass correlation coefficients of the PL lengths obtained by the three specialists were greater than 0.997. This MRI technique provides highly stable and repeatable *in vivo* data of PL and ACL geometry relevant to ACL reconstruction surgery with PL grafts.

Key words: Magnetic resonance imaging; Patellar tendon; Anterior cruciate ligament; Technical optimization

INTRODUCTION

Reconstructing the distal one-third of the patellar ligament (PL) under arthroscopy has become a standard operation for treating anterior cruciate ligament (ACL) injury (Chang et al., 2003). Numerous clinical applications have proven that failing to recognize factors such as ligament shortening or other lesions in the ligaments, bone fractures in the operative zone, and lesions in the meniscus or articular cartilage could lead to failure of the operation. Moreover, without adequate immobilization of the implant, prolonged implantation could also result in implant tunnel mispairing (Barber, 2000; Mariani et al., 2003). Therefore, obtaining detailed information regarding ligament geometry related to the operation and accurately monitoring implant fixation are important.

Magnetic resonance imaging (MRI) has excellent tissue and space resolution, and has been applied in knee examinations. The patella, femur, tibia, and ACL can be visualized clearly using MRI, which provides distinct contrast against the surrounding tissues. Thus, MRI could be used to determine ligament geometry and the details of the knee joint.

Reported data regarding ACL length determination in China vary markedly mainly because ACL data are obtained from cadavers, and only ACL lengths are provided by the Constitution Committee of the Chinese Society for Anatomical Sciences (CSAS) (Huang and Liu, 2000). MRI investigations of the PL are also based on abnormal situations (Insall and Salvati, 1971; Kartus et al., 1999; Shalaby and Almekinders, 1999), and the adopted methods vary because of the different starting points of the investigations. In this study, MRI was technically optimized to examine the geometry between the PL and ACL.

SUBJECTS AND METHODS

The study included 157 healthy volunteers including 79 men aged 15 to 71 years (average, 40.96 ± 19.65 years), with average weight and height of 64.24 ± 4.98 kg and 169.63 ± 6.06 cm, respectively, and 78 women aged 15 to 73 years (average, 43.06 ± 19.68 years), with average weight and height of 56.93 ± 4.88 kg and 158.73 ± 4.52 cm, respectively.

Inspection equipment and positioning

A USA GE Signa 1.5-T superconducting MRI system with a special surface coil was used. The volunteers lay supine with their knees in a suitable position to center the coil at the lower edge of the patella.

ACL scanning

The ACL lies along an inclined sagittal plane (Figure 1). The detailed procedure was as follows: 1) Fast spoiled gradient-recalled (FSPGR) MRI was used to scan the knee simultaneously along three planes (coronal, sagittal, and axial). 2) Using the axial view of the intercondylar fossa of the femur, a tangent line was drawn along the posterior aspect of the medial and external condyles, followed by a vertical line from the center of the intercondylar fossa. 3) The inclined sagittal line was positioned along the inner side of the vertical line at an angle of 10° to 15°. A fast spin echo (FSE) sequence was then used to obtain a high-resolution T1-weighted image (H-T1WI) of the ACL. The parameters were as follows: echo time (TE), 10 ms; repetition time (TR), 575 ms; echo train length (TL), 2; bandwidth (BW), 20.83: field of view (FOV), 16; slice thickness (ST), 4 mm; spacing, 1 mm; frequency encoding (Freq), 384; phase encoding (Phase), 256; number of excitations (Nex), 2.

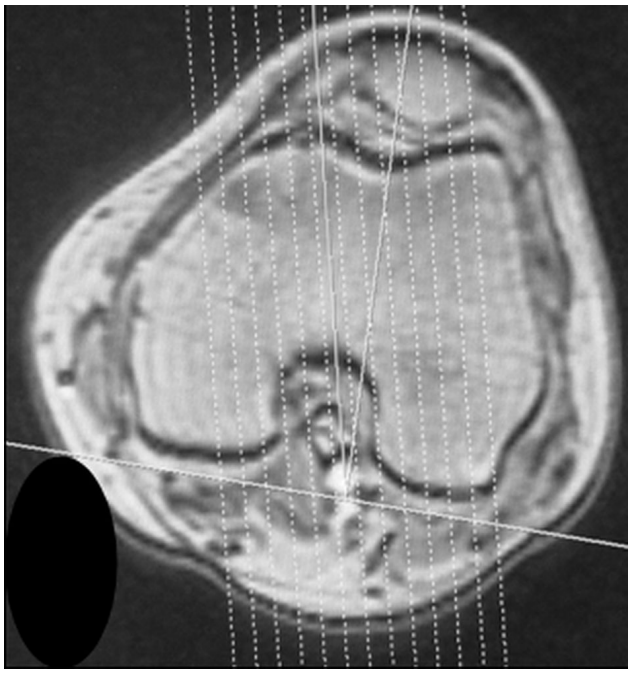

Figure 1. Scan method of the anterior cruciate ligament.

PL scanning

PL scanning was then performed. The PL vertical view image was positioned in a sagittal orientation. The patella and the tibial tubercle were included in the range. The sagittal view scan line of the PL was then defined by the vertical view image centered midway between the lower edge of the patella and the tibial tubercle (Figure 2). The H-T1WI parameters were as follows: TE, 10 ms; TR, 650 ms; TL, 2; BW, 20.83; FOV, 16; ST, 4 mm; spacing, 1

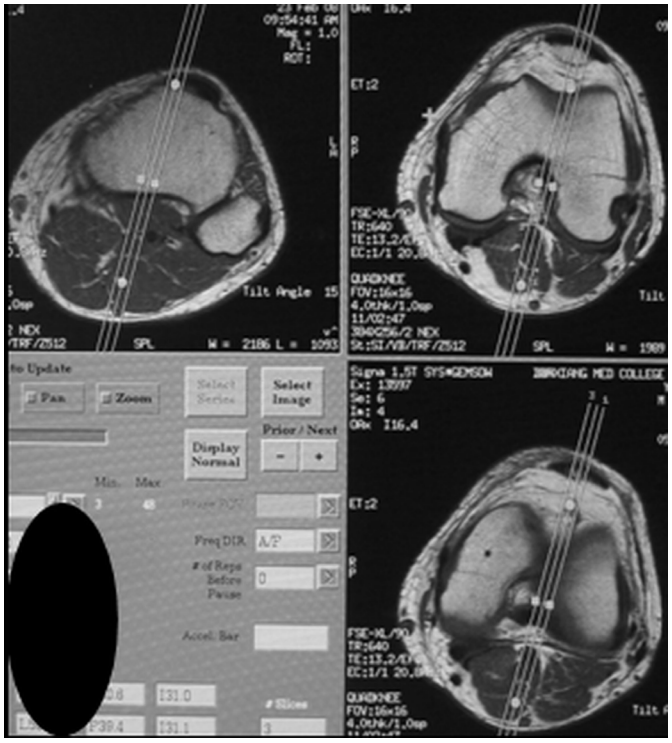

Figure 2. Scan methods of the patellar ligament.
mm; Freq, 384; Phase, 256; Nex, 2.

Measurement and analysis of the PL and ACL

The length of the PL (L1) was defined as the distance from the lower edge of the patella to the tibial tubercle (Figure 3). The length of the ACL (L2) was defined as the distance from the femoral attachment of the ACL, which is the highest point of the intercondylar fossa, to the front facies ossea of the intercondylar eminence, the tibial attachment point (line B1B2, Figure 4). All measurements from the MRI were obtained with the same standards and determined using the Radworks 5.1 workstation. An image diagnostician (A) determined the initial reliability of the data. After 1 month, an image diagnostician (B) and an orthopaedist (C) measured the left L1. The intraclass correlation coefficient (ICC) was calculated using the same workstation to test data reliability. All data were analyzed using SPSS 13.0, and a paired *t*-test was performed to analyze the same left and right knee joint ligament indices. An independent sample *t*-test was conducted to compare the indices between genders. $P < 0.05$ was considered to be statistically significant.

RESULTS

The total lengths of the ACL and the PL that fulfilled the clinical determination re-

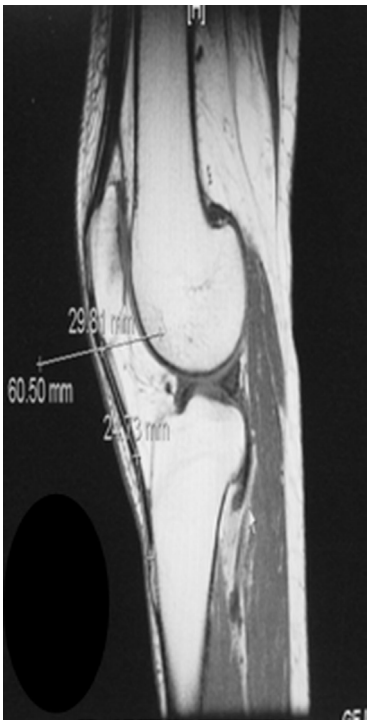

Figure 3. Length determination of the anterior cruciate and patellar ligaments.

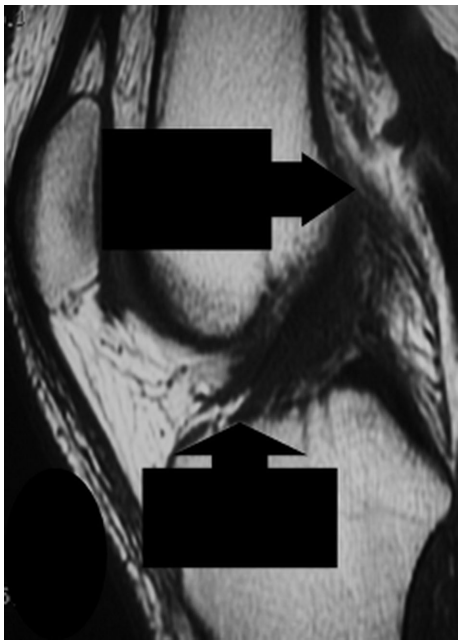

Figure 4. Length determination of the anterior cruciate ligament.

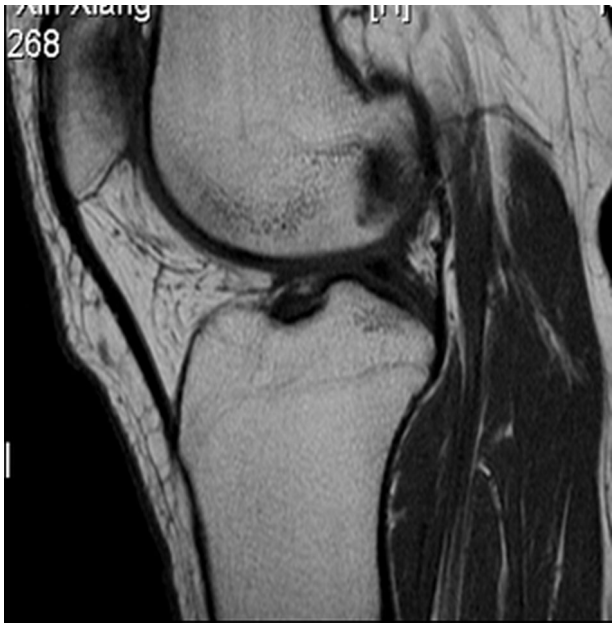

Figure 5. Normal patellar ligament with sagittal view of total length.

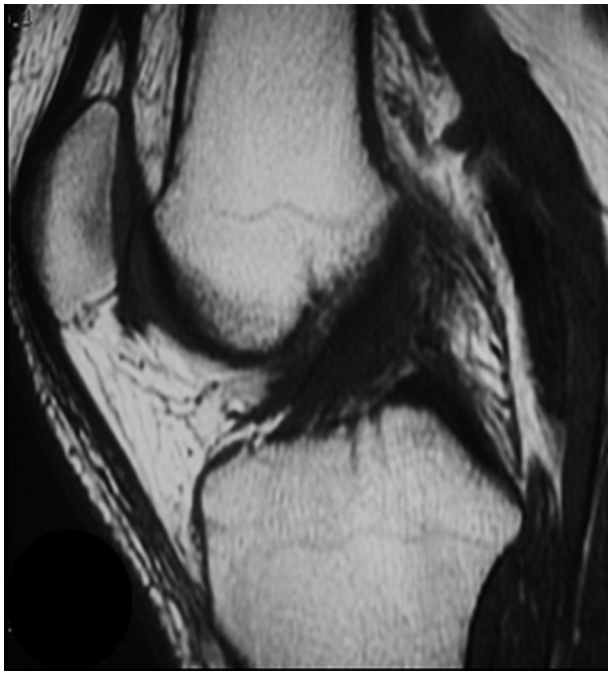

Figure 6. Normal anterior cruciate ligament with sagittal view of total length.

quirements were obtained (Figures 5 and 6). The acquisition time was 2.4 min.

PL and ACL lengths differed significantly between genders. PL and ACL lengths did not differ significantly between left and right knees. The average ACL and PL lengths in male subjects were 36.98 ± 4.12 and 42.20 ± 4.21 mm, respectively. By contrast, the average ACL and PL lengths in female subjects were 40.15 ± 4.00 and 35.80 ± 4.67 mm, respectively (Tables 1 and 2).

The ICCs of the left PL length determined by three specialists (A, B, C) were greater than 0.997 (Table 3).

Table 1. Comparison of MRI data of left and right patellar (PL) and anterior cruciate ligaments (ACL).

	Left data (mm)	Right data (mm)	*t*-value	P
N	157	157		
PL length	41.15 ± 4.24	41.21 ± 4.23	-1.97	0.05
ACL length	36.40 ± 4.44	36.38 ± 4.45	1.39	0.17

Table 2. MRI data of patellar (PL) and anterior cruciate ligaments (ACL) of different gender.

Tissue	Male		Female		*t*-value	P
	N	Data (mm)	N	Data (mm)		
PL						
Left	79	42.19 ± 4.22	78	40.10 ± 4.01**	3.18	0.00
Right	79	42.20 ± 4.23	78	40.20 ± 4.02**	3.04	0.00
Sum	158	42.20 ± 4.21	156	40.15 ± 4.00**	4.41	0.00
ACL						
Left	79	36.99 ± 4.12	78	35.80 ± 4.68	1.70	0.09
Right	79	36.96 ± 4.14	78	35.79 ± 4.69	1.64	0.10
Sum	158	36.98 ± 4.12	156	35.80 ± 4.67	2.26	0.03

Table 3. Intraclass correlation coefficient of 3 left patellar ligament length.

	Detector A (mm)	Detector B (mm)	Detector C (mm)
Detector A	1.000	1.000	0.997
Detector B	1.000	1.000	0.997
Detector C	0.997	0.997	1.000

DISCUSSION

MRI, which has good tissue and spatial resolution, can be used to clearly visualize osseous and soft tissue structures such as the patella, femur, tibia, and PL. MRI provides clear boundaries against the surrounding tissues, and the entire PL can theoretically be visualized if the scan plane is parallel to the ligament. He et al. (2008) and Chen et al. (2008) used 0.2 T MRI to acquire ligament images. In the current study, we used 1.5 T MRI with a special surface coil. Measurements using Radworks 5.1 had an accuracy of 0.01 mm. The ligaments were able to be scanned even when they were curved (Figure 3). In addition, the ICCs of the left PL lengths obtained by three specialists (A, B, C) were all greater than 0.997. Therefore, the reliability of the data obtained using Radworks 5.1 was acceptable. Moreover, the ACL lengths of the subjects were close to the data provided by the CSAS (36.00 ± 0.20 mm), also

indicating data reliability.

The pathological and histological changes in different diseases have different theoretical bases and MRI features. In recent years, MRI has enabled detection of features that could lead to the failure of the ACL reconstruction operation of the distal one-third of the PL, such as ligament shortening or other lesions, bone fractures in the operative zone, and lesions in the meniscus or articular cartilage.

Hydrogen atoms are fixed in the dense mesh formed by polypeptides in normal ligaments. These atoms are visualized in MRI as low signals in any ligament sequence (Beltran et al., 1987). In damaged ACLs, ACL tears are indicated by continuous breaks, relaxation, thickenings, crude borders, lumps, and significant increases in partial signals, and indirect indicators include increased tibial antelocation angle, edema of the soft tissue surrounding the ACL, changes in bone architecture, and meniscopathy in other ligaments (Niitsu et al., 1995). The nonsynovium-coated area of the ACL (Higueras Guerrero et al., 1999), as well as bruises or fractures of the femur and tibia, particularly those with corresponding contralateral bruises in the tibia and femur (Stein et al., 1995), appears as edema. Increased PL signal intensity, continuous breaks, increased thickness, and PL shortening are observed in dysplasias.

Numerous MRI methods for examining the knee are available. The main sequences used in clinics are as follows: spin echo sequence, FSE sequence, fat-suppression sequence, gradient echo sequence, echo planar imaging sequence, high-resolution MRI, and 3-D Fourier-transformation imaging and dynamic MRI (Harms et al., 1989; Kojima et al., 1996). T1WI is recommended in the spin echo sequence (Yoo et al., 2007), which requires T1- and T2-weighted sequences in normal ligament MRI scans. Normally, some other forms of T2 weighting, such as T2* and short TI inversion recovery sequencing, are used to compensate for T2-weighting limitations. However, some specialized sequences are unsuitable. ACL patients normally have low tolerance, requiring faster scanning speeds. In this study, we used FSPGR and H-T1WI with FSE to obtain the ACL position as images in three planes. This method satisfies the determination requirements and substantially shortens the scanning time.

The ability of MRI scans to distinguish tissues depends mainly on the signal-to-noise ratio (S/N), spatial resolution, and tissue-signal intensity ratio (Adam et al., 1991; Foo et al., 1992; Potte et al., 1998).

The pulse sequence, coil design, and continuous development of the gradient field continually increase the resolution of the PL in MRI. Increasing the intensity of the gradient field and prolonging the time duration also greatly improve the image resolution. All of these results are based on decreasing S/N at different degrees. The relative importance of TE effects depends on the T2 relaxation of the focused tissue, with the acceptance that BW decreases with a specified FOV and matrix. Therefore, shorter TE sequences should be applied in tissues with shorter T2 to achieve better S/N.

Increasing the gradient pulse duration time for higher resolution and lower BW decreases the noise when a shorter TE is necessary. This improvement is achievable using standard MRI hardware (1-G/cm gradient field), although the adjustment shortens the S/N of tissue with a shorter T2. Two methods shorten T2: changing the gradient field form from the normal half-sine echo to a rhombus formation and obtaining a partial echo, specifically by obtaining symmetrical echoes (about 60%) to synthesize the rest of the images artificially. For tissues with very short T2s, the S/N changes caused by the increased signal intensity exceed those caused by the increased noise. Increasing the gradient field can also be used to shorten the TE, but the increased BW would also increase the noise. Thus, a high gradient intensity (>4 G/cm)

can only be achieved using instruments with small local gradient coils.

A GE Signa 1.5-T superconducting MRI system with a special surface coil was used in the current experiment. The FSE-T1WI parameters for high-resolution sagittal view images of the ligaments were as follows: TE, 10 ms; TR, 575 ms; TL, 2; BW, 20.83; FOV, 16; ST, 4 mm; spacing, 1 mm; Freq, 384; Phase, 256; Nex, 2. The T1WI obtained completely satisfies the determination requirements, and is 2 min shorter than the usual SE sequences for normal scanning.

The ACL extends backwards, upwards, and outwards from the front of the tibial intercondylar eminence, forming an angle with the sagittal plane. Li et al. (1997) designated this angle as the "side obliquity". According to the projection theory, the side obliquity between the ACL and the sagittal plane is the posterolateral "inherent side obliquity" that has an average angle of 28.80 ± 9.80°. Therefore, the ACL sagittal plane at the anatomic fault is shown well. Chen et al. (2008) used 0.2 T MRI to investigate the differences between normal knees and frozen ones. The investigation revealed that the inclined ACL coronal plane is parallel to the direction of the slice. Recently, an inclined sagittal plane scan was classified as a routine scan, increasing the rate mainly by positioning the patient's knee at 10° to 15° abduction and decreasing the scan thickness to 3 mm to position the MRI scan plane parallel to the ACL axis (Arndt et al., 1996). A 1.5-T MRI system with a special knee coil was used in this study. Moreover, the inclined sagittal plane was 10° to 15° from the vertical line of the tail-skirt tangent line of the inside and outside femur. The ST used was 4 mm, and 100% of the normal ACL was shown in one layer.

The distal one-third of the PL is very important in ACL reconstruction. Miller and Oiszewski (1997) and Huang and Liu (2000) reported a few *in vivo* cases wherein the determination tools were not computerized. Yoo et al. (2007) and He et al. (2008) used sagittal plane images to determine the patellar central plane of the PL. The position of the femur was not fixed, such that the plane examined in this view was actually the PL gravity plane. The CSAS has not provided reference data for PL length, given that PL length varies greatly. The measurements in this research all focused on the line from the apex of the patella to the central point of the tibial tubercle and depended on the high contrast, high resolution, and multiplanar capabilities of MRI. All of the relative data for clinical PL transplantation were obtained *in vivo*.

CONCLUSIONS

A 1.5-T MRI system and Radworks 5.1 workstation were combined to optimize ACL and PL scanning without invasive procedures. This setup could provide important information for ACL reconstruction surgery. The Radworks 5.1 workstation exhibited minimal dependence on the subjects, which enabled acquisition of data with high reliability and repeatability.

Conflicts of interest

The authors declare no conflict of interest.

REFERENCES

Adam G, Nolte-Ernsting C, Prescher A, Bühne M, et al. (1991). Experimental hyaline cartilage lesion: two-dimensional spin-echo versus three-dimensional gradient-echo MR imaging. *J. Magn. Reson. Imaging* 1: 665-672.

Arndt WF 3rd, Truax AL, Barnett FM, Simmons GE, et al. (1996). MR diagnosis of bone contusions of the knee: comparison of coronal T2-weighted fast spin echo with fat saturation and fast spin echo STIR images with conventional STIR images. *AJR Am. J. Roentgenol.* 166: 119-124.

Barber FA (2000). Flipped patellar tendon autograft anterior cruciate ligament reconstruction. *Arthroscopy* 16: 483-490.
Beltran J, Noto AM, Herman LJ and Lubbers LM (1987). Tendons: high-field-strength, surface coil MR imaging. *Radiology* 162: 735-740.
Chang SK, Egami DK, Shaieb MD, Kan DM, et al. (2003). Anterior cruciate ligament reconstruction: allograft versus autograft. *Arthroscopy* 19: 453-462.
Chen W, Lu M, Wang J, Ding SY, et al. (2008). The comparative study of the anterior cruciate ligament in oblique coronal thin anatomical section and MRI. *Chin. J. Radiol.* 42: 80-83.
Foo TK, Shellock FG, Hayes CE, Schenck JF, et al. (1992). High-resolution MR imaging of the wrist and eye with short TR, short TE, and partial-echo acquisition. *Radiology* 183: 277-281.
Harms SE, Flamig DP, Fisher CF and Fulmer JM (1989). New method for fast MR imaging of the knee. *Radiology* 173: 743-750.
He CA, Lou LX, Guo Z, Liang W, et al. (2008). Length Ratio of Patellar Tendon and Patella Measured on MR Images. *Radiol. Practice* 6: 670-672.
Higueras Guerrero V, Torregrosa Andrés A, Martí-Bonmatí L, Casillas C, et al. (1999). Synovialisation of the torn anterior cruciate ligament of the knee: comparison between magnetic resonance and arthroscopy. *Eur. Radiol.* 9: 1796-1799.
Huang HY and Liu JF (2000). The length of transfer cruciate ligament from patellar ligament and its significance. *Chin. J. Clin. Anat.* 18: 19-20.
Insall J and Salvati E (1971). Patella position in the normal knee joint. *Radiology* 101: 101-104.
Kartus J, Lindahl S, Stener S, Eriksson BI, et al. (1999). Magnetic resonance imaging of the patellar tendon after harvesting its central third: a comparison between traditional and subcutaneous harvesting techniques. *Arthroscopy* 15: 587-593.
Kojima KY, Demlow TA, Szumowski J and Quinn SF (1996). Coronal fat suppression fast spin echo images of the knee: evaluation of 202 patients with arthroscopic correlation. *Magn. Reson. Imaging* 3: 1017-1022.
Li RX, Wu DY, Li MZ, Chen QW, et al. (1997). A study of the azimuths of the anterior cruciate ligament and their function significance. *Chin. J. Sports Med.* 16: 101-103.
Mariani PP, Calvisi V and Margheritini F (2003). A modified bone-tendon-bone harvesting technique for avoiding tibial tunnel-graft mismatch in anterior cruciate ligament reconstruction. *Arthroscopy* 19: E3.
Miller MD and Oiszewski AD (1997). Cruciate ligament graft intra-articular distance. *Arthroscopy* 3: 291-293.
Niitsu M, Kuramochi M, Anno I and Itai Y (1995). Secondary signs of anterior cruciate ligament tear at MR imaging. *Nippon Igaku Hoshasen Gakkai Zasshi* 55: 375-379.
Potte HG, Linkiater JM, Allen AA, Hannafin JA, et al. (1998). Magnetic resonance imaging of articular cartilage in the knee. An evaluation with use of fast-spin-echo imaging. *J. Bone Joint Surg. Am.* 80: 1276-1284.
Shalaby M and Almekinders LC (1999). Patellar tendinitis: the significance of magnetic resonance imaging findings. *Am. J. Sports Med.* 27: 345-349.
Stein LN, Fischer DA, Fritts HM and Quick DC (1995). Occult osseous lesions associated with anterior cruciate ligament tears. *Clin. Orthop. Relat. Res.* (313): 187-193.
Yoo JH, Yi SR and Kim JH (2007). The geometry of patella and patellar tendon measured on knee MRI. *Surg. Radiol. Anat.* 29: 623-628.

